ChemComm

# A microfluidic organic transistor for reversible and real-time monitoring of $H_2O_2$ at ppb/ppt levels in ultrapure water


| | |
|---|---|
| Journal: | *ChemComm* |
| Manuscript ID | CC-COM-02-2022-001224.R1 |
| Article Type: | Communication |
| | |

COMMUNICATION

# A microfluidic organic transistor for reversible and real-time monitoring of $H_2O_2$ at ppb/ppt levels in ultrapure water

Received 00th January 20xx,
Accepted 00th January 20xx

DOI: 10.1039/x0xx00000x

Kohei Ohshiro [a], Yui Sasaki [a], Qi Zhou [a], Pierre Didier [a,b], Takasuke Nezaki [c], Tomoharu Yasuike [c], Masao Kamiko [a] and Tsuyoshi Minami [a, b,*]

**A microfluidic organic transistor functionalized with phenylboronic acid firstly succeeded in reversible and real-time monitoring of $H_2O_2$ at ppb/ppt levels in ultrapure water, which would be used not only as portable chemical sensors but also as monitoring tools to clarify unknown reaction mechanisms of phenylboronic acid with $H_2O_2$.**

Hydrogen peroxide ($H_2O_2$) is yielded as a by-product by UV irradiation in the process of ultrapure water manufacturing, which could cause oxidative decomposition of an ion exchange resin utilized for ultrapure water.[1] In addition, oxidation corrosion of metals in a semiconductor manufacturing process could be induced by the over-standard levels of $H_2O_2$ in ultrapure water.[2] Therefore, the monitoring of $H_2O_2$ plays a significant role in maintaining the purity of ultrapure water. To this date, various methods for $H_2O_2$ detection by colorimetric[3] and redox titrations[4] and fluorescent probes[5] have been developed, while many of those sensitivities are not satisfied for $H_2O_2$ monitoring at ppb levels. Given the fact that the concentration of $H_2O_2$ in ultrapure water (< 3 ppb) is defined by the International Roadmap for Device and Systems (IRDS),[6] the development of highly sensitive and real-time detection methods is required in industrial applications.

Phenylboronic acid (PBA)[7] is converted into phenol by oxidation with $H_2O_2$.[8] The oxidation reaction occurs through the formation of a boronate anion, followed by the hydrolysis to phenol in the presence of water. Thus, the response of chemical sensors could be switched quantitatively by time-dependent structural changes of PBA derivatives. Indeed, PBA-based chemosensors have successfully detected $H_2O_2$, whereas real-time monitoring of $H_2O_2$ is still challenging.[9] The unfeasible continuous detection of $H_2O_2$ is presumably attributed to the control difficulty of chemical reactions between PBA derivatives and $H_2O_2$. Therefore, an appropriate sensor design to control inherent features of PBA derivatives is a key for the realization of real-time detection of $H_2O_2$.

An organic field-effect transistor (OFET) is an attractive organic electronic device comprising a self-assembled π-conjugated material, which displays non-linear electrical characteristics by applying gate and drain voltages to each electrode.[10] The characteristics of OFETs are appropriately manipulated by changes in the dipole moment of self-assembled monolayers (SAMs) for dielectric layers.[11] As another role of SAMs, the membranes can be used as recognition scaffolds on the gate electrode[12] or the semiconductive layer[13] for chemical sensing, which achieve highly sensitive detection owing to their well-packed interface.[12a,12b,14] However, chemical sensing on the semiconductive layer of the OFET is still concerned because of instability of the semiconductive material to water.[13a] Thus, an extended-gate-type OFET was employed for the sensing manner[15] in this study. We decided to modify 4-mercaptophenylboronic acid (4-MPBA)[16] as the SAM-based recognition portion toward highly sensitive detection of $H_2O_2$ on the extended-gate electrode. In the irreversible process, the

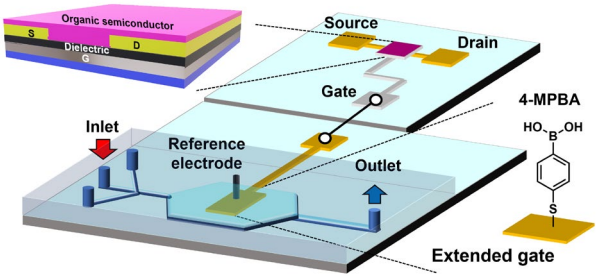


**Fig. 1** Schematic illustration of the microfluidic system with the extended-gate-type OFET sensor for $H_2O_2$ detection. The detection portion was functionalized with 4-MPBA.

[a] *Institute of Industrial Science, The University of Tokyo, 4-6-1 Komaba, Meguro-ku, Tokyo, 153-8505, Japan; E-mail: tminami@iis.u-tokyo.ac.jp*
[b] *LIMMS/CNRS-IIS(UMI2820),The University of Tokyo, 4-6-1 Komaba, Meguro-ku, Tokyo, 153-8505, Japan*
[c] *Kurita Water Industries Ltd., 4-10-1 Nakano, Nakano-ku, Tokyo, 164-0001, Japan*
†Electronic Supplementary Information (ESI) available: Fabrication details of the extended-gate-type OFET-based sensor and the microfluidic chamber, characterization of the extended-gate electrode by LSV, PYS and XPS, DFT calculation of dipole moment, and selectivity test. See DOI: 10.1039/x0xx00000x

conversion of the PBA derivative into the phenol structure causes the decrease of the dipole moment,[16a] which could change transistor characteristics in static measurements. In the case of continuous measurements, the transistor characteristics could be real-timely controlled by the generation of negative charges derived from the formation of the boronate anion with $H_2O_2$. Thus, the introduction of PBA-based SAM into the OFET would be a potent approach for highly sensitive and real-time detection of $H_2O_2$. The extended-gate electrode (Au) functionalized with 4-MPBA was further incorporated into a microfluidic chamber,[17] allowing continuous $H_2O_2$ detection (Fig. 1).

The $H_2O_2$ detection portion was formed by immersion of the extended-gate electrode into a methanol solution containing 4-MPBA. Linear sweep voltammetry (LSV)[18] was applied to evaluate a molecular density of 4-MPBA on the Au electrode, which was estimated to be (2.0 ± 0.1) × $10^{-9}$ mol/cm$^2$ in three repetitions (Fig. S2†). The estimated low error indicated that the highly reproducible fabrication of the detection portion was achieved. For the OFET fabrication, poly{2,5-bis(3-tetradecylthiophene-2yl)thieno[3,2-b]thiophene} (PBTTT-C14) was employed as a semiconductive material owing to its easy-to-obtain interdigitated packing structure by a wetting process.[19] By employing a fluorinated polymer material (*i.e.*, CYTOP™) for a passivation layer, the transistor characteristics of the extended-gate-type OFET were successfully evaluated even under ambient conditions. In this regard, the basic parameters manufactured OFET such as field-effect mobility and an on/off ratio were estimated to be 2.1×$10^{-3}$ cm$^2$/Vs and $10^3$, respectively. Further fabrication of the extended-gate-type OFET was summarized in ESI†. In this assay, the detectability of the OFET-based chemical sensor was examined in an ultrapure water sample (*i.e.*, Milli-Q water) toward industrial applications. Fig. 2 displays a titration isotherm obtained by changes in transfer characteristics upon the addition of $H_2O_2$ (0-100 pg/mL). The LoD of the OFET-based chemical sensor was determined to be 0.71 pg/mL (= ppt), estimated by the 3σ method with the average value of $V_{TH}$ (Fig. 2, inset).[20] Remarkably, the estimated LoD was lower than those of electrochemical,[21] colorimetric[22] and fluorescent[23] methods (Table S1†). In addition, the sensitivity of the OFET-based sensor implied the satisfaction of the requirement of the $H_2O_2$ concentration defined by IRDS. In this regard, negative shifts of the transfer curves were observed by a static measurement (Fig. S3†) with an increase of the $H_2O_2$ concentration, which was probably due to the change in the chemical structure of the PBA derivative to the phenol structure accompanied by the changes in the dipole moments. Certainly, each $V_{TH}$ of the OFET functionalized with 4-MPBA and 4-hydroxybenzene thiol (4-HBT) was estimated to be −0.94 V and −1.10 V, respectively, indicating that the above-mentioned negative shifts of the transistor characteristics were derived from the oxidation of the PBA derivative. To support the changes in the transistor characteristics stemmed from the reaction to $H_2O_2$, the selectivity test was demonstrated against oxidizing agents such as benzoyl peroxide (BPO), 2,3-dichloro-5,6-dicyano-1,4-benzoquinone (DDQ), *tert*-butyl hydroperoxide (*t*-BHP), sodium nitrate, and sodium hypochlorite (Fig. 3).

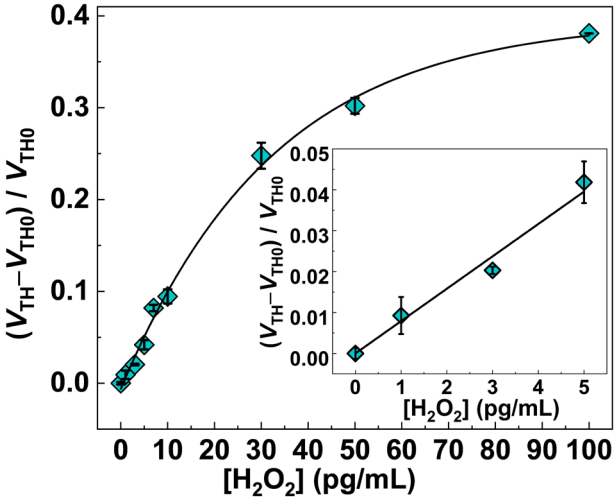


**Fig. 2** Electrical detection of $H_2O_2$ (0–100 pg/mL) in ultrapure water by the static measurement using the extended-gate-type OFET functionalized with 4-MPBA. The electrical measurement at each concentration was carried out after the incubation of the extended-gate into the sample solution for 5 min. The titration isotherm was obtained by gathering of the calculated threshold voltages ($V_{TH}$s) in the transfer characteristics at $V_{DS}$ = −1 V. The $V_{TH0}$ and the $V_{TH}$ represent threshold voltages before and after adding $H_2O_2$, respectively. Inset exhibits the lower end of the titration.

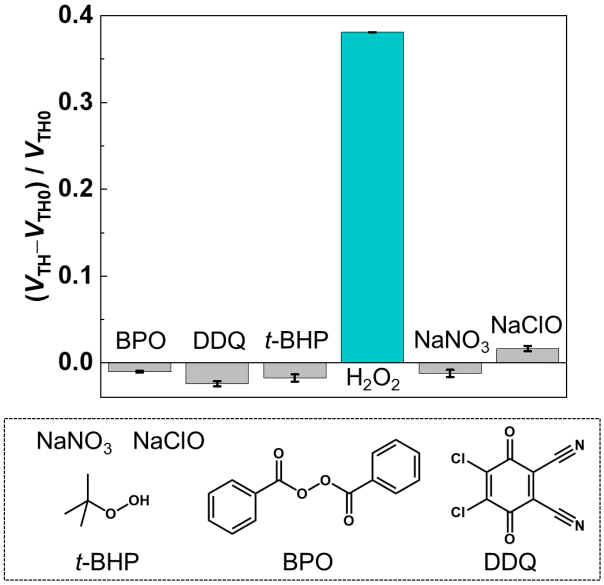


**Fig. 3** Selectivity test for benzyl peroxide (BPO), 2,3-dichloro-5,6-dicyano-1,4-benzoquinone (DDQ), *tert*-butyl hydroperoxide (*t*-BHP), $H_2O_2$, sodium nitrate ($NaNO_3$), and sodium hypochlorite (NaClO) in ultrapure water. [Analyte] = 100 pg/mL.

Indeed, the observed highest response of the OFET to $H_2O_2$ suggested that the oxidation of the PBA derivatives by $H_2O_2$ induced the shifts of the transistor characteristics.

Next, DFT calculation was carried out to investigate the changes in the dipole moments derived from the oxidation of the PBA derivative by adding $H_2O_2$. The dipole moments of 4-MPBA and 4-HBT were estimated to be 4.2D and 1.3D, respectively, which revealed a higher magnitude of the dipole

moment of 4-MPBA than that of 4-HBT (Fig. S7†). According to a correlation of dipole moments of 1,4-substituted thiophenol derivatives and their work functions, the changes in the work functions of Au electrodes depend on the magnitude of dipole moments of monolayers on the Au electrodes.[24] Therefore, photoelectron yield spectroscopy (PYS) in air was performed to evaluate the work function of extended-gate electrodes. As shown in Fig. S8†, each work function of the Au electrodes functionalized with 4-MPBA and 4-HBT were estimated to be 4.9 eV and 5.0 eV, respectively. The correlation tendency between the dipole moments of the SAMs and the work functions of the modified electrodes matched with the reported relationship.[24] Moreover, by the treatment of $H_2O_2$, the work function of the 4-MPBA modified-electrode shifted from 4.9 eV to 5.0 eV. The work function of the Au electrode with 4-MPBA by oxidation corresponded to that of 4-HBT. Given the fact that the changes in the work function after the treatment of $H_2O_2$, the shifts of the transistor characteristics upon the addition of $H_2O_2$ attributed to the change in the dipole moment derived from the conversion of the PBA derivative into the phenol structure. Furthermore, a decrease of a peak intensity of B 1*s* in the 4-MPBA attached electrode after the $H_2O_2$ treatment was observed by the X-ray photoelectron spectroscopy (XPS) measurement, which also suggested the $H_2O_2$ reaction on the SAM (Fig. S9(B)†). On the other hand, the remain of B 1*s* in Fig. S9(B)† implied that an unreacted PBA form still existed. In other words, the reversible structural changes between the PBA derivative and the boronate anion[25] before the full conversion into the phenol derivative could be controlled by a reaction time using the microfluidic device.

The real-time monitoring of $H_2O_2$ was finally carried out using the OFET integrated with the microchamber. The design of the microfluidic chamber made of poly(dimethylsiloxane) was optimized by using COMSOL Multiphysics software, allowing a uniform flow of water by the appropriate parameters such as length, thickness, and shape of channels and chamber, and flow rate. The details of the fabrication scheme were summarized in the ESI†.[12c] The integrated OFET with the microfluidic chamber exhibited the stepwise change of the drain current ($I_{DS}$), which corresponded to the increase of $H_2O_2$ concentration (Fig. S6). Moreover, the microfluidic OFET-based sensor displayed an increase and decrease of $I_{DS}$ upon the alternative injection of $H_2O_2$ and ultrapure water (Fig. 4). The observed reversible change of $I_{DS}$ was probably due to the dynamic structural change to the boronate anion with $H_2O_2$.[25] This is the first demonstration to achieve the reversible monitoring of $H_2O_2$ by using PBA derivatives. Next, the changes in the microfluidic OFET characteristics by the continuous flow of $H_2O_2$ were monitored to investigate the robustness of the PBA derivative-based SAM on the extended-gate electrode. For this purpose, a high concentration of $H_2O_2$ (10 ppm) was injected. The microfluidic OFET showed an increase of $I_{DS}$ by flowing $H_2O_2$, and the $I_{DS}$ was maximized within 40 s. After this period, the $I_{DS}$ was gradually decreased by the continuous flow of $H_2O_2$, and 80% decrease of the $I_{DS}$ value from the maximized $I_{DS}$ was observed within 20 min. Taking into consideration the incubation time of PBA derivatives with $H_2O_2$ (3.4 ppm) for oxidation in the recent report,[9a] the observed response time was reasonable. Notably, the reversible response was not observed after the long-term flow of $H_2O_2$, implying that the microfluidic OFET could monitor not only the reversible boronate anion with $H_2O_2$ but also the irreversible conversion into the phenol structure.

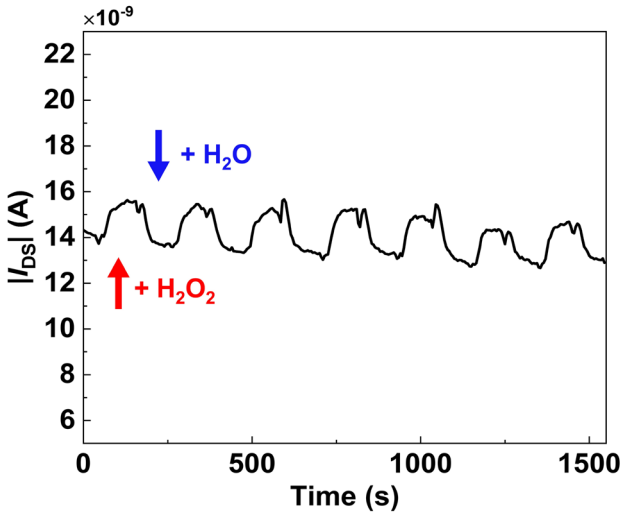


**Fig. 4** Real-time monitoring of $H_2O_2$ (10 ppb) in ultrapure water utilizing the extended-gate-type OFET with the microfluidic chamber. Continuous flow was applied at 46 μL/min.

In summary, the extended-gate-type OFET sensor integrated with the microchamber was developed for the highly sensitive and real-time detection of $H_2O_2$ in ultrapure water. The changes in the transfer characteristics in the static $H_2O_2$ detection were induced by the conversion of the PBA derivative into the phenol structure, which was accompanied by the change in the dipole moment. The quantitative changes in the OFET characteristics provided the LoD value (0.71 pg/mL), satisfying the requirement of the $H_2O_2$ concentration defined by IRDS.[6] Most importantly, the microfluidic OFET device firstly succeeded in the reversible and real-time monitoring of $H_2O_2$. We believe that our microfluidic system functionalized with artificial receptors would be used not only as portable chemical sensors but also as monitoring tools to clarify unknown reaction mechanisms of chemical reactions.

TM gratefully acknowledgments the financial support from the Japan Society for the Promotion of Science (JSPS KAKENHI Grant Numbers JP21H01780, JP20K21204, and JP20H05207), Core-to-Core Program, and JST CREST (Grant No. JPMJCR2011).

## Conflicts of interest

There are no conflicts of interest to declare.

## Notes and references

1. J. M. Campos-Martin, G. Blanco-Brieva and J. L. G. Fierro, *Angew. Chem. Int. Ed.*, 2006, **45**, 6962-6984.
2. T. Miyazawa, T. Terachi, S. Uchida, T. Satoh, T. Tsukada, Y. Satoh, Y. Wada and H. Hosokawa, *J. Nucl. Sci. Technol.*, 2006, **43**, 884-895.

3. Review, see: (a) (a) M. Lee, B. G. Heikes and D. W. O'Sullivan, *Atmos. Environ.*, 2000, **34**, 3475-3494. Examples, see: (b) G. Eisenberg, *Ind. Eng. Chem., Anal. Ed.*, 1943, **15**, 327-328; (c) S. Wu, S. Y. Tan, C. Y. Ang, Z. Luo and Y. Zhao, *Chem. Commun.*, 2016, **52**, 3508-3511; (d) S. Feng, M. Ming, M. Wang, X. Wang, D. He, P. Jiang and Y. Chen, *Chem. Commun.*, 2020, **56**, 12347-12350; (e) E. Dervisevic, N. H. Voelcker, G. Risbridger, K. L. Tuck and V. J. Cadarso, *Anal. Chem.*, 2022, **94**, 1726-1732.
4. Review, see: (a) (a) W. Chen, S. Cai, Q.-Q. Ren, W. Wen and Y.-D. Zhao, *Analyst*, 2012, **137**, 49-58; (b) K. Wang, J. Huang, H. Chen, Y. Wang and S. Song, *Chem. Commun.*, 2020, **56**, 12109-12121. Examples, see: (c) Y.-A. Woo, H.-R. Lim, H.-J. Kim and H. Chung, *J. Pharm. Biomed.*, 2003, **33**, 1049-1057; (d) L. Jiang, I. Santiago and J. Foord, *Chem. Commun.*, 2017, **53**, 8332-8335; (e) Y. Ni, H. Liu, D. Dai, X. Mu, J. Xu and S. Shao, *Anal. Chem.*, 2018, **90**, 10152-10158.
5. (a) X. Sun, K. Lacina, E. C. Ramsamy, S. E. Flower, J. S. Fossey, X. Qian, E. V. Anslyn, S. D. Bull and T. D. James, *Chem. Sci*, 2015, **6**, 2963-2967; (b) S. Ye, N. Hananya, O. Green, H. Chen, A. Q. Zhao, J. Shen, D. Shabat and D. Yang, *Angew. Chem. Int. Ed.*, 2020, **59**, 14326-14330; (c) Y. Ning, Y. Huo, H. Xue, Y. Du, Y. Yao, A. C. Sedgwick, H. Lin, C. Li, S.-D. Jiang, B.-W. Wang, S. Gao, L. Kang, J. L. Sessler and J.-L. Zhang, *J. Am. Chem. Soc.*, 2020, **142**, 10219-10227; (d) Z. Wu, M. Liu, Z. Liu and Y. Tian, *J. Am. Chem. Soc.*, 2020, **142**, 7532-7541; (e) S. Li, P. Wang, W. Feng, Y. Xiang, K. Dou and Z. Liu, *Chem. Commun.*, 2020, **56**, 1050-1053.
6. IEEE, "International Roadmap for Devices and Systems 2018 update, Yield Enhancement", https://irds.ieee.org/images/files/pdf/2018/2018IRDS_YE.pdf, (accessed Febrary 28, 2022).
7. (a) R. Nishiyabu, Y. Kubo, T. D. James and J. S. Fossey, *Chem. Commun.*, 2011, **47**, 1106-1123; (b) Z. Guo, I. Shin and J. Yoon, *Chem. Commun.*, 2012, **48**, 5956-5967; (c) A. P. Davis, in *Supramolecular Chemistry in Water*, 2019, DOI: https://doi.org/10.1002/9783527814923.ch5, pp. 161-191.
8. (a) X. Sun, S.-Y. Xu, S. E. Flower, J. S. Fossey, X. Qian and T. D. James, *Chem. Commun.*, 2013, **49**, 8311-8313; (b) S. Gupta, P. Chaudhary, L. Seva, S. Sabiah and J. Kandasamy, *RSC Adv.*, 2015, **5**, 89133-89138; (c) B. L. Patenall, G. T. Williams, L. Gwynne, L. J. Stephens, E. V. Lampard, H. J. Hathaway, N. T. Thet, A. E. Young, M. J. Sutton, R. D. Short, S. D. Bull, T. D. James, A. C. Sedgwick and A. T. A. Jenkins, *Chem. Commun.*, 2019, **55**, 15129-15132.
9. (a) B. Gatin-Fraudet, R. Ottenwelter, T. Le Saux, S. Norsikian, M. Pucher, T. Lombès, A. Baron, P. Durand, G. Doisneau, Y. Bourdreux, B. I. Iorga, M. Erard, L. Jullien, D. Guianvarc'h, D. Urban and B. Vauzeilles, *Proc. Natl. Acad. Sci. U.S.A.*, 2021, **118**, e2107503118; (b) B. J. Graham, I. W. Windsor, B. Gold and R. T. Raines, *Proc. Natl. Acad. Sci. U.S.A.*, 2021, **118**, e2013691118.
10. (a) G. Horowitz, *Adv. Mater.*, 1998, **10**, 365-377; (b) J. Mei, Y. Diao, A. L. Appleton, L. Fang and Z. Bao, *J. Am. Chem. Soc.*, 2013, **135**, 6724-6746; (c) H. Chen, W. Zhang, M. Li, G. He and X. Guo, *Chem. Rev.*, 2020, **120**, 2879-2949.
11. (a) K. P. Pernstich, S. Haas, D. Oberhoff, C. Goldmann, D. J. Gundlach, B. Batlogg, A. N. Rashid and G. Schitter, *J. Appl. Phys*, 2004, **96**, 6431-6438; (b) M. Salinas, C. M. Jäger, A. Y. Amin, P. O. Dral, T. Meyer-Friedrichsen, A. Hirsch, T. Clark and M. Halik, *J. Am. Chem. Soc.*, 2012, **134**, 12648-12652; (c) F. Gholamrezaie, A.-M. Andringa, W. S. C. Roelofs, A. Neuhold, M. Kemerink, P. W. M. Blom and D. M. de Leeuw, *Small*, 2012, **8**, 241-245.
12. Review, see: (a) (a) R. Kubota, Y. Sasaki, T. Minamiki and T. Minami, *ACS Sens.*, 2019, **4**, 2571-2587; (b) F. Torricelli, D. Z. Adrahtas, Z. Bao, M. Berggren, F. Biscarini, A. Bonfiglio, C. A. Bortolotti, C. D. Frisbie, E. Macchia, G. G. Malliaras, I. McCulloch, M. Moser, T.-Q. Nguyen, R. M. Owens, A. Salleo, A. Spanu and L. Torsi, *Nat. Rev. Dis. Primers*, 2021, **1**, 66. Examples, see: (c) P. Didier, N. Lobato-Dauzier, N. Clément, A. J. Genot, Y. Sasaki, É. Leclerc, T. Minamiki, Y. Sakai, T. Fujii and T. Minami, *ChemElectroChem*, 2020, **7**, 1332-1336; (d) T. Minamiki, T. Minami, Y.-P. Chen, T. Mano, Y. Takeda, K. Fukuda and S. Tokito, *Commun. Mater.*, 2021, **2**, 8.
13. (a) M. E. Roberts, S. C. B. Mannsfeld, N. Queraltó, C. Reese, J. Locklin, W. Knoll and Z. Bao, *Proc. Natl. Acad. Sci. U.S.A.*, 2008, **105**, 12134-12139; (b) Y. Jang, M. Jang, H. Kim, S. J. Lee, E. Jin, J. Y. Koo, I.-C. Hwang, Y. Kim, Y. H. Ko, I. Hwang, J. H. Oh and K. Kim, *Chem*, 2017, **3**, 641-651; (c) T. Minamiki, Y. Hashima, Y. Sasaki and T. Minami, *Chem. Commun.*, 2018, **54**, 6907-6910.
14. (a) H. Li, W. Shi, J. Song, H.-J. Jang, J. Dailey, J. Yu and H. E. Katz, *Chem. Rev.*, 2019, **119**, 3-35; (b) J. Wang, D. Ye, Q. Meng, C.-a. Di and D. Zhu, *Adv. Mater. Technol.*, 2020, **5**, 2000218.
15. (a) P. Bergveld, *Sens. Actuators B Chem.*, 2003, **88**, 1-20; (b) T. Minamiki, T. Minami, R. Kurita, O. Niwa, S.-i. Wakida, K. Fukuda, D. Kumaki and S. Tokito, *Appl. Phys. Lett.*, 2014, **104**, 243703.
16. (a) D. Barriet, C. M. Yam, O. E. Shmakova, A. C. Jamison and T. R. Lee, *Langmuir*, 2007, **23**, 8866-8875; (b) T. Minami, T. Minamiki, Y. Hashima, D. Yokoyama, T. Sekine, K. Fukuda, D. Kumaki and S. Tokito, *Chem. Commun.*, 2014, **50**, 15613-15615.
17. (a) T. Someya, A. Dodabalapur, A. Gelperin, H. E. Katz and Z. Bao, *Langmuir*, 2002, **18**, 5299-5302; (b) S. P. White, S. Sreevatsan, C. D. Frisbie and K. D. Dorfman, *ACS Sens.*, 2016, **1**, 1213-1216; (c) S. Ricci, S. Casalini, V. Parkula, M. Selvaraj, G. D. Saygin, P. Greco, F. Biscarini and M. Mas-Torrent, *Biosens. Bioelectron.*, 2020, **167**, 112433.
18. O. Azzaroni, M. E. Vela, G. Andreasen, P. Carro and R. C. Salvarezza, *J. Phys. Chem. B*, 2002, **106**, 12267-12273.
19. (a) I. McCulloch, M. Heeney, C. Bailey, K. Genevicius, I. MacDonald, M. Shkunov, D. Sparrowe, S. Tierney, R. Wagner, W. Zhang, M. L. Chabinyc, R. J. Kline, M. D. McGehee and M. F. Toney, *Nat. Mater.*, 2006, **5**, 328-333; (b) B. S. Ong, Y. Wu, Y. Li, P. Liu and H. Pan, *Chem. Eur. J.*, 2008, **14**, 4766-4778.
20. J. N. Miller and J. C. Miller, *Statistics and Chemometrics for Analytical Chemistry, Pearson/Prentice Hall, Upper Saddle River, N.J.*, 2005.
21. (a) X. Gan, T. Liu, J. Zhong, X. Liu and G. Li, *ChemBioChem*, 2004, **5**, 1686-1691; (b) K.-C. Fang, C.-P. Hsu, Y.-W. Kang, J.-Y. Fang, C.-C. Huang, C.-H. Hsu, Y.-F. Huang, C.-C. Chen, S.-S. Li, J. Andrew Yeh, D.-J. Yao and Y.-L. Wang, *Biosens. Bioelectron.*, 2014, **55**, 294-300; (c) L. G. Bach, M. L. N. Thi, N. T. Son, Q. B. Bui, H. T. Nhac-Vu and P. H. Ai-Le, *J. Electroanal. Chem.*, 2019, **848**, 113359; (d) G. Zhiguo, Y. Shuping, L. Zaijun, S. Xiulan, W. Guangli, F. Yinjun and L. Junkang, *Anal. Chim. Acta*, 2011, **701**, 75-80; (e) S. Manavalan, J. Ganesamurthi, S.-M. Chen, P. Veerakumar and K. Murugan, *Nanoscale*, 2020, **12**, 5961-5972; (f) H. Wang, W. Chen, Q. Chen, N. Liu, H. Cheng and T. Li, *J. Electroanal. Chem.*, 2021, **897**, 115603.
22. (a) T. Zhang, S. Zhang, J. Liu, J. Li and X. Lu, *Anal. Chem.*, 2020, **92**, 3426-3433; (b) H. Chen, Q. Shi, G. Deng, X. Chen, Y. Yang, W. Lan, Y. Hu, L. Zhang, L. Xu, C. Li, C. Zhou, Y. She and H. Fu, *Sens. Actuators B Chem.*, 2021, **343**, 130104.
23. T. Lin, Y. Qin, Y. Huang, R. Yang, L. Hou, F. Ye and S. Zhao, *Chem. Commun.*, 2018, **54**, 1762-1765.
24. A. Tada, Y. Geng, M. Nakamura, Q. Wei, K. Hashimoto and K. Tajima, *Phys. Chem. Chem. Phys.*, 2012, **14**, 3713-3724.
25. H. G. Kuivila and A. G. Armour, *J. Am. Chem. Soc.*, 1957, **79**, 5659-5662.

 